Energy-Efficient Antenna Sharing and Relaying for Wireless Networks

J. Nicholas Laneman and Gregory W. Wornell

Research Laboratory of Electronics
Massachusetts Institute of Technology
Cambridge, MA 02139 USA

Abstract—We develop energy-efficient transmission protocols for wireless networks that exploit spatial diversity created by antenna sharing: coordinated transmission and/or processing by several distributed radios. We focus on singleuser transmission and examine several possibilities for the strategy employed by the assisting radio, or relay, including decoding and forwarding as well as amplifying and forwarding. In each case, we develop receivers based upon maximum-likelihood and/or maximum signal-to-noise ratio criteria, relate their structures, and compare their bit-error probability performance by means of analysis and simulations. We cast singlehop and multihop routing into our framework for comparison purposes. All of our antenna sharing protocols offer diversity gains over single- and multi-hop transmission, and our results suggest that low-complexity amplifying and forwarding is energy-efficient in spite of noise amplification at the relay.

I. INTRODUCTION

Relaying information over several point-to-point communication links is a basic building block of communication networks. Such relaying is utilized in wired and wireless networks to achieve higher network connectivity (broader coverage), efficient utilization of resources such as power and bandwidth, better economies of scale in the cost of long-haul transmissions (through traffic aggregation), interoperability among networks, and more easily manageable, hierarchical network architectures.

In wireless networks, direct transmission between widely separated radios can be very expensive in terms of transmitted power required for reliable communication. High-power transmissions lead to faster battery drain (shorter network life) as well as increased interference at nearby radios. As alternatives to direct transmission, there are two basic and frequently-employed examples of relayed transmission for wireless networks. In cellular settings, for example, networks provide connectivity between low-power mobiles by providing local connections to high-power basestations that are relayed via a wireline basestation network. In sensor networks, and military battlefield communication networks in general, the use of wireline infrastructure is often precluded and the radios may be substantially power constrained; for these ad-hoc or peer-to-peer networks, transmissions can be relayed wirelessly. As these examples suggest, relayed transmission enlists two or more radios to perform multiple transmissions. The end-to-end transmissions potentially incur higher delay, but because the individual transmissions are over shorter distances (in the wireless case), or over high-quality cabling (in the wireline case), the
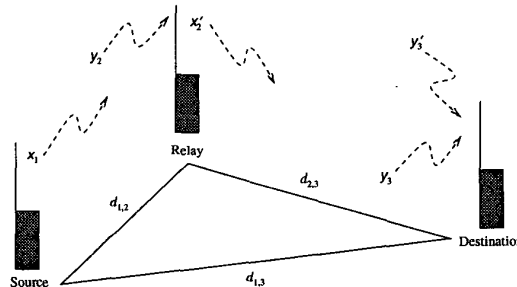
Fig. 1. Example three-radio (sub)network for which relaying protocols, and especially, antenna sharing, or diversity, protocols can be motivated and developed. Indicated are the transmitted signals x_1 and x_2', the received signals y_2, y_3, and y_3', and the radio separations $d_{i,j}$.

power requirements for reliable communication can be much lower.

The basic relaying protocols described above are constructed from the sequential use of point-to-point links, where the links are essentially viewed at the network protocol layer; however, more general approaches are possible that involve the coordination of *both* the direct and relayed transmissions, at the network and lower protocol layers, and correspond to scenarios to which the classical relay channel model [1] applies. In this paper, we develop energy-efficient relaying protocols that create and exploit spatial diversity to combat fading due to multipath propagation, a particularly severe form of interference experienced in wireless networks.

To illustrate the main concepts, we consider the simple wireless network depicted in Fig. 1. We focus specifically on transmissions from radio 1, called the source, to radio 3, called the destination, with the possibility of employing radio 2 as a relay. At the physical layer, the destination receives potentially useful signals from all transmitters that are active, and may combine multiple transmissions of the same signal to reduce variations in performance caused by signal fading, a technique referred to broadly as spatial diversity combining [2]. We refer to this form of spatial diversity as *antenna sharing*, in contrast to the currently more conventional forms of spatial diversity [3], because the radios essentially share their antennas and other resources to create a "virtual array" through distributed transmission and signal processing.

After developing a mathematical model in Section II for the network in Fig. 1, we scratch the surface of the rich set of de-

sign issues and options that arise in the context of antenna sharing and relaying for wireless networks. Section III casts the basic relaying protocols, referred to as singlehop and multihop transmission, respectively, into our framework, and explores a number of possibilities for antenna sharing protocols, in terms of what signals the source and relay jointly transmit as well as how the relay and destination jointly process signals. Performance comparisons, and simulation results in Section IV, suggest that antenna sharing transmission protocols are capable of overcoming the noisy channels between the distributed radio antennas to achieve diversity gain and outperform singlehop and multihop transmission in a variety of scenarios of interest.

II. SYSTEM MODEL

In our model for the three-radio wireless network depicted in Fig. 1, narrowband transmissions suffer the effects of path loss and flat fading as arise in e.g., slow-frequency-hop networks. Our analysis focuses on the case of slow fading to isolate the benefits of spatial diversity alone; however, we emphasize at the outset that our results extend naturally to the kinds of highly mobile scenarios in which faster fading is encountered.

Our baseband-equivalent, discrete-time channel model for the network in Fig. 1 consists of two subchannels, orthogonal in, e.g., adjacent time slots or frequencies. This decomposition is necessary because practical limitations in radio implementation prevent the relay from simultaneously transmitting and receiving on the same channel. On the first subchannel, the source transmits a sequence $x_1[n]$, with average sample energy 1, and the relay and destination receive signals

$$y_2[n] = a_{1,2} \sqrt{\mathcal{E}_1} \, x_1[n] + z_2[n],$$ (1)

$$y_3[n] = a_{1,3} \sqrt{\mathcal{E}_1} \, x_1[n] + z_3[n],$$ (2)

respectively. On the second subchannel, the relay transmits a sequence $x_2'[n]$, with average sample energy ≤ 1, and the destination receives[1]

$$y_3'[n] = a_{2,3} \sqrt{\mathcal{E}_2} \, x_2'[n] + z_3'[n].$$ (3)

Here $a_{i,j}$ captures the effects of path loss and static fading on transmissions from radio i to radio j, $\mathcal{E}_i$ is the transmitted energy of radio i, and $z_j[n]$ and $z_3'[n]$ model additive receiver noise and other forms of interference.

Statistically, we model the fading coefficients $a_{i,j}$ as zero-mean, mutually independent complex jointly Gaussian random variables with variances $\sigma_{a_{i,j}}^2$, and we model the additive noises $z_j[n]$ and $z_3'[n]$ as zero-mean, mutually independent, white complex jointly Gaussian sequences with variance $\mathcal{N}_0$. We define the signal-to-noise ratio (SNR) in each received signal as $\gamma_{i,j} \triangleq |a_{i,j}|^2 \mathcal{E}_i / \mathcal{N}_0$; under the Rayleigh fading model,

[1] We employ the notation "$(\cdot)'$" to distinguish the signals on the second subchannel from those on the first; the fading coefficients $a_{i,j}$ are the same because the subchannels are assumed to be adjacent and the fading is flat across frequency.
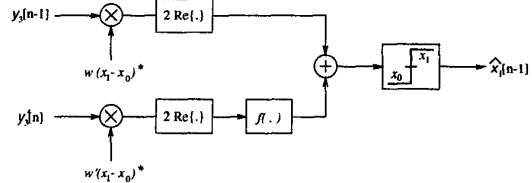

Fig. 2. Destination receiver structure.

the SNRs are independent exponential random variables with expected values $\overline{\gamma}_{i,j} \triangleq \mathrm{E}\,[\gamma_{i,j}] = \sigma_{a_{i,j}}^2 \, \mathcal{E}_i / \mathcal{N}_0$.

III. TRANSMISSION PROTOCOLS

Within the physical layer framework described in Section II, we examine several protocols that support transmission between the source and destination. Each protocol consists of a source modulation format, a relay processing/modulation scheme, and a destination receiver structure.

For simplicity of exposition, we treat coherently-detected, constant-modulus binary transmissions, so that the source transmitted signal $x_1[n]$ is white and takes values x_0 and x_1 with equal probability. To enable coherent detection, the relay and destination receivers must first obtain, via training sequences in the protocol headers, accurate estimates of the link fading coefficients; in several scenarios, the destination also utilizes an estimate of $\gamma_{1,2}$. We assume these estimates are perfect in our preliminary analysis.

All of our destination receiver structures can be implemented as shown in Fig. 2. This "combiner" can be viewed as a generalized matched-filter, or maximum-ratio combiner, suitably modified to fit the protocol. As we will see, qualitative comparisons among the various transmission protocols can be made by examining their respective weights w and w' as well as their mappings $f(\cdot)$.

A. Singlehop Transmission

Singlehop transmission, often referred to as singlehop routing in the ad-hoc networking community [4], consists of direct transmission between the source and destination radios. In this case, the source transmits $x_1[n]$, the relay transmits $x_2'[n] = 0$, i.e., nothing, and the destination processes only (2).

Minimum probability of error (MPE) detection corresponds to conditional MPE detection for each value of the fading coefficient $a_{1,3}$. Since the input symbols are equally likely, conditional MPE detection corresponds to conditional maximum-likelihood (ML) detection; this can be implemented by the combiner in Fig. 2 with any mapping $f(\cdot)$ and weights

$$w = \frac{a_{1,3}^* \sqrt{\mathcal{E}_1}}{\mathcal{N}_0}, \qquad w' = 0,$$ (4)

i.e., the destination ignores $y_3'[n]$. Since the equivalent channel is conditionally Gaussian with SNR $\gamma_{1,3}$, the conditional error

8

probability for singlehop transmission can be obtained from standard Gaussian results [2]

$$P_{\mathrm{SH}|\gamma_{1,3}} = Q\left(\sqrt{(1-\rho)\gamma_{1,3}}\right), \qquad (5)$$

where $Q(t) = \frac{1}{\sqrt{2\pi}} \int_t^\infty e^{-s^2/2} ds$, and ρ is a constant depending upon the modulation format. For example, coherently-detected BPSK has $\rho = -1$, while coherently-detected FSK has $\rho = 0$. The average error performance of singlehop transmission, P_{SH}, follows by averaging (5) over the exponential probability density function for $\gamma_{1,3}$; the result can be approximated for large (average) SNR by [2]

$$P_{\mathrm{SH}} \approx \frac{1}{K\,\overline{\gamma}_{1,3}}, \qquad \overline{\gamma}_{1,3} \gg 1, \qquad (6)$$

where K is another constant depending upon the modulation format. For example, coherently-detected BPSK has $K = 4$, while coherently detected FSK has $K = 2$.

B. Multihop Transmission

The basic wireless relaying protocol qualitatively described in Section I is called multi-hop routing in the ad-hoc networking community [4]. Multi-hop transmission in our framework can be viewed as cascading singlehop transmission between the source and relay with singlehop transmission between the relay and destination. Specifically, the source transmits $x_1[n]$, and the relay forms an estimate $\check{x}_1[n]$ from (1). The relay transmits this estimate as $x_2'[n] = \check{x}_1[n-1]$. Finally, the destination forms an estimate $\hat{x}_1[n-1]$ of $x_1[n-1]$ from (3). The sample delay accounts for processing and (relative) propagation delay through the relay.

As we will develop, ML detection of $x_1[n]$ at the relay is preferable. We examine two destination receivers for multihop transmission. The first forms ML estimates of the relay's transmitted signal $x_2'[n]$, and is useful for developing average error performance bounds. The second makes ML estimates of the source transmitted sequence $x_1[n-1]$.

B.1 ML Detection of $x_2'[n]$

Conditional ML detection of $x_2'[n]$ corresponds to the single-hop ML detector from Section III-A, with the rolls of $y_3[n-1]$ and $y_3'[n]$ swapped. Specifically, the conditional ML detector can be implemented as the combiner in Fig. 2 with

$$w = 0, \qquad w' = \frac{a_{2,3}^* \sqrt{\mathcal{E}_2}}{\mathcal{N}_0}, \qquad f(t) = t. \qquad (7)$$

If the relay decision process can be modeled as a binary-symmetric channel (BSC) with crossover probability ϵ depending upon the SNR $\gamma_{1,2}$, the conditional error probability in estimating $x_1[n-1]$ at the combiner specified by (7) can be upper bounded by

$$P_{\mathrm{MH}|\gamma_{1,2},\gamma_{2,3}} \leq \epsilon + P_{\mathrm{SH}|\gamma_{2,3}}, \qquad (8)$$

where the first term arises from the event that the relay makes a decision error, and the second term arises from the event that the destination makes a decision error given that the relay does not. The result (8) suggests that MPE detection of $x_1[n]$ at the relay is preferable. In this case, $\epsilon = P_{\mathrm{SH}|\gamma_{1,2}}$, and the average error performance can be approximated for large SNR by [2]

$$P_{\mathrm{MH}} \leq \frac{1}{K\,\overline{\gamma}_{1,2}} + \frac{1}{K\,\overline{\gamma}_{2,3}}, \qquad \overline{\gamma}_{1,2}, \overline{\gamma}_{2,3} \gg 1. \qquad (9)$$

As we will see in Section IV, this bound is tight in several regimes of interest.

B.2 ML Detection of $x_1[n-1]$

Conditional ML detection of $x_1[n-1]$ at the destination is somewhat more involved, but can also be implemented as a combiner in the form of Fig. 2. Again, assuming the relay decision process can be modeled as a BSC with crossover probability ϵ, some algebra shows that the destination conditional ML detector of $x_1[n-1]$ has

$$w = 0, \quad w' = \frac{a_{2,3}^* \sqrt{\mathcal{E}_2}}{\mathcal{N}_0}, \quad f(t) = \ln\left[\frac{\epsilon + (1-\epsilon)e^t}{\epsilon e^t + (1-\epsilon)}\right]. \quad (10)$$

The key step in obtaining (10) lies in the expanding the likelihood $p(y_3'|a_{2,3}, x_1)$ by averaging over whether or not the relay makes a decision error, i.e.,

$$p\left(y_3' | a_{2,3}, x_1 = x_0\right) = (1 - \epsilon)\, p\left(y_3' | a_{2,3}, \check{x}_1 = x_0\right) \\ + \epsilon\, p\left(y_3' | a_{2,3}, \check{x}_1 = x_1\right),$$

for $x = x_0$, and similarly for $x = x_1$. The results (10) follows after substitution of the conditional Gaussian likelihoods, taking the log-likelihood ratio, and algebraic simplifications.

Limiting arguments indicate, and Fig. 3 exhibits, that the mapping $f(t)$ in (10) essentially "clips" its input to the values $\pm \ln[\epsilon/(1 - \epsilon)]$ and is approximately linear between these extremes for small t. For $\epsilon < 1/2$, the mappings in (7) and (10) satisfy $f(t) \geq 0$ for $t \geq 0$ and $f(t) < 0$ for $t < 0$; hence, their symbol estimates for uncoded transmissions will be identical. Consequently, as we have seen previously, ML detection at the relay is preferable, and the average error performance of this multihop protocol should also be well approximated by (9). Finally, we observe that as $\epsilon \to 1/2$, the mapping $f(t)$ in (10) goes to 0, and if the destination fixes $\epsilon = 0$ in the detector, i.e., it does not explicitly take into account the uncertainty of the relay decisions, (10) reduces to (7).

Although apparently irrelevant for uncoded multihop transmission, we will see in Section III-C that the clipping property of $f(t)$ in (10) is significant in the context of diversity transmission. More generally, while clipping the matched-filter output may be irrelevant for uncoded transmissions, it is important for coded systems (with symbol-by-symbol detection employed at the relay), because it limits the contribution of any one symbol's log-likelihood, e.g., branch metric in a Viterbi algorithm, to the sum of the log-likelihoods, e.g., path metric in a Viterbi algorithm.
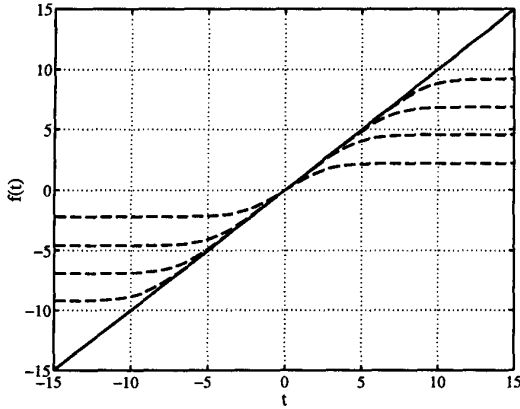
9

Fig. 3. Combiner mapping $f(t)$ from (10). Successively higher dashed curves (for $t > 0$) correspond to $\epsilon = 10^{-1}, 10^{-2}, \ldots, 10^{-4}$, respectively. For comparison, the solid curve corresponds to the linear mapping $f(t) = t$.

C. Diversity Transmission with Decoding Relay

Our first diversity transmission protocol combines singlehop and multihop transmission to create and exploit spatial diversity. Specifically, our protocol for diversity transmission with a decoding relay consists of the following. The source transmits $x_1[n]$ to both the relay and destination on the subchannel (1) and (2). The relay forms an estimate of $x_1[n]$ from its received signal $y_2[n]$, and transmits this estimate, delayed by one sample to account for processing and (relative) propagation delay, as $x_2'[n]$ on subchannel (3). As throughout Section III-B, we assume the relay decision process can be modeled as a BSC with crossover probability ϵ, and based upon reasoning similar to that discussion, we employ ML detection at the relay.

The destination estimates $x_1[n-1]$ from both its received signals (2) and (3). When suitably combined, the chances of both signals exhibiting deep fading is reduced; therein lies the diversity benefit. The challenge in this setting is to design a detector that can overcome the effects of uncertainty in the relay decisions and still exploit the available spatial diversity.

C.1 ML Detection of $x_1[n-1]$

Combining the results of Section III-A and Section III-B, conditional ML detection of $x_1[n-1]$ from both (2) and (3) can be implemented as the combiner in Fig. 2 with

$$w = \frac{a_{1,2}^* \sqrt{\mathcal{E}_1}}{\mathcal{N}_0}, \quad w' = \frac{a_{2,3}^* \sqrt{\mathcal{E}_2}}{\mathcal{N}_0}, \quad f(t) = \ln\left[\frac{\epsilon + (1-\epsilon)e^t}{\epsilon e^t + (1-\epsilon)}\right]. \tag{11}$$

Here the clipping effect of $f(t)$ in (11) is more important than it was for uncoded multihop transmission. The nonlinearity in $f(t)$ increasingly reduces, with increasing ϵ, the contribution of the diversity branch through the relay.

If the destination assumes the relay decisions are always correct, then (11) with $\epsilon \to 0$ becomes a conventional maximum-

ratio combiner

$$w = \frac{a_{1,2}^* \sqrt{\mathcal{E}_1}}{\mathcal{N}_0}, \quad w' = \frac{a_{2,3}^* \sqrt{\mathcal{E}_2}}{\mathcal{N}_0}, \quad f(t) = t. \tag{12}$$

This combiner, though mismatched in general, performs reasonably well for small ϵ. Similar to the bound in Section III-B.1, we can upper bound the average error performance of the detector corresponding to (12), again using large SNR approximations from [2], by

$$P_{\mathrm{DD}} \leq \frac{1}{K\,\overline{\gamma}_{1,2}} + \frac{3}{K^2\,\overline{\gamma}_{1,3}\,\overline{\gamma}_{2,3}}, \quad \overline{\gamma}_{1,2}, \overline{\gamma}_{1,3}, \overline{\gamma}_{2,3} \gg 1. \tag{13}$$

The first term in (13) arises from the event that the relay makes a decision error, and the second term arises from the event that the destination makes a decision error given that the relay does not, corresponding to a conventional transmit antenna diversity scenario [3]. This bound is only useful for approximating the performance of the ML detector (11) in channel environments for which $\overline{\gamma}_{1,2}$ is especially large, e.g., when the relay is very close to the source.

C.2 Maximum SNR Detector

As an alternative design criterion, we determine the receiver that maximizes the SNR of the slicer input. To arrive at this max SNR receiver, we examine the relay decision $\check{x}_1 = x_1 + e$, where e is a random variable capturing the effects of decision errors. A few calculations yield

$$E\left[e|x_1\right] = \begin{cases} \epsilon(x_1 - x_0) & \text{if } x_1 = x_0 \\ \epsilon(x_0 - x_1) & \text{if } x_1 = x_1 \end{cases},$$

$$\sigma_e^2 = \epsilon(1 - \epsilon)|x_1 - x_0|^2.$$

Letting $\tilde{x}_1 = x_1 + E\left[e|x_1\right]$, and $\tilde{e} = e - E\left[e|x_1\right]$, the relay estimate $\check{x}_1 = \tilde{x}_1 + \tilde{e}$ can be viewed as equally-likely symbols drawn from the constant-magnitude constellation

$$\begin{aligned} \tilde{x}_1 &= (1 - \epsilon)\,x_1 + \epsilon\,x_0, \\ \tilde{x}_0 &= (1 - \epsilon)\,x_0 + \epsilon\,x_1, \end{aligned} \tag{14}$$

plus an additive noise that is uncorrelated with $\tilde{x}_1$, having mean zero and variance σ_e^2. Thus, the two signals received by the destination may be written as

$$\begin{aligned} y_3[n-1] &= a_{1,3}\sqrt{\mathcal{E}_1}\,x_1[n-1] + z_3[n-1], \\ y_3'[n] &= a_{2,3}\sqrt{\mathcal{E}_2}\,(\check{x}[n-1] + \tilde{e}[n-1]) + z_3'[n]. \end{aligned} \tag{15}$$

Observing that $(\tilde{x}_1 - \tilde{x}_0) = (1 - 2\epsilon)(x_1 - x_0)$, the maximum SNR destination receiver, a matched-filter for (15), can be implemented as the combiner in Fig. 2 with

$$w = \frac{a_{1,3}^* \sqrt{\mathcal{E}_1}}{\mathcal{N}_0}, \quad w' = \frac{a_{2,3}^* \sqrt{\mathcal{E}_2}(1 - 2\epsilon)}{|a_{2,3}|^2 \mathcal{E}_2 \sigma_e^2 + \mathcal{N}_0}, \tag{16}$$

$$f(t) = t.$$

10

Examining w' in (16) more closely, we see that it consists of the maximum-ratio combiner weight w' in (12) followed by the linear mapping

$$f(t) = \frac{(1 - 2\epsilon)}{\gamma_{2,3}\,\sigma_e^2 + 1}\,t. \qquad (17)$$

For $\epsilon \to 1/2$, (17) goes to zero, indicating that the maximum SNR detector ignores the received signal y_3' just as the ML detector defined by (11). Like the ML detector, (16) converges to the maximum-ratio combiner (12) for $\epsilon \to 0$.

We conclude this section by noting that [5] develops results similar to (11) and (16) in the context of cellular networks. Specifically, the linear detector in [5] corresponds to the combiner in Fig. 2 with

$$w = \frac{a_{1,3}^* \sqrt{\mathcal{E}_1}}{\mathcal{N}_0}, \quad w' = \lambda \frac{a_{2,3}^* \sqrt{\mathcal{E}_2}}{\mathcal{N}_0}, \quad f(t) = t;$$

the parameter λ is chosen numerically to minimize the conditional error probability of this linear detector.

D. Diversity Transmission with Amplifying Relay

In the previous section, we explored several destination detection algorithms assuming the relay employed ML detection. If we constrain the relay to employ linear processing, i.e., amplifying, alternative transmission protocols result. We might expect this constraint to induce excessive noise amplification, but, as the simulation results in Section IV suggest, a destination ML detector designed for an amplifying relay can be quite competitive, and perhaps even outperform the transmission protocols from the previous section, when the relay is close to the destination.

Our protocol for diversity transmission with an amplifying relay consists of the following. The source transmits $x_1[n]$ to both the relay and destination on the subchannel (1) and (2). The relay transmits an amplified (and delayed) version of its received sequence, i.e., $x_2'[n] = \beta y_2[n-1]$ on the subchannel (3). To decode symbol $x_1[n-1]$, the destination processes its two received signals

$$\begin{aligned} y_3[n-1] &= a_{1,3}\,x_1[n-1] + z_3[n-1], \\ y_3'[n] &= a_{2,3}\,\beta\,\left(a_{1,2}\,x_1[n-1] + z_2[n-1]\right) + z_3'[n]. \end{aligned} \qquad (18)$$

The destination conditional ML detector of $x_1[n-1]$ from (18) can be implemented as the combiner in Fig. 2 with

$$w = \frac{a_{1,3}^* \sqrt{\mathcal{E}_1}}{\mathcal{N}_0}, \quad w' = \frac{a_{2,3}^* \beta^* \, a_{1,2}^* \sqrt{\mathcal{E}_1}}{(|a_{2,3}|^2 |\beta|^2 + 1)\mathcal{N}_0}, \qquad (19)$$
$$f(t) = t.$$

To satisfy its output power constraint, the relay amplifier can operate at a maximum gain satisfying

$$|\beta|^2 = \frac{\mathcal{E}_2}{|a_{1,2}|^2 \mathcal{E}_1 + \mathcal{N}_0}, \qquad (20)$$

where we allow the gain to depend upon the fading realization $a_{1,2}$ from the source to the relay. Substituting (20) into (19), we see that the channel is conditionally Gaussian with SNR that can be manipulated into the form $\gamma_{1,3} + \gamma_{\text{eq}}$, where

$$\gamma_{\text{eq}}^{-1} = \gamma_{1,2}^{-1} + \gamma_{2,3}^{-1} + \gamma_{1,2}^{-1}\gamma_{2,3}^{-1}. \qquad (21)$$

The conditional bit-error probability can be readily computed using standard Gaussian results, yielding

$$P_{\text{DA}|\gamma_{1,3},\gamma_{1,2},\gamma_{2,3}} = Q\left(\sqrt{(1 - \rho)\left[\gamma_{1,3} + \gamma_{\text{eq}}\right]}\right). \qquad (22)$$

Note that the conditional error probability (22) exhibits a sum of SNRs as we might expect in a diversity scenario.

Examining (21), we see that

$$\gamma_{\text{eq}} < \gamma_{\min} \triangleq \min\left\{\gamma_{1,3},\ \gamma_{2,3}\right\}. \qquad (23)$$

Since $\gamma_{1,3}$ and $\gamma_{2,3}$ are independent exponential random variables in our model, their minimum is also exponential with expected value satisfying

$$\overline{\gamma}_{\min}^{-1} = \overline{\gamma}_{1,3}^{-1} + \overline{\gamma}_{2,3}^{-1}, \qquad (24)$$

analogous to a parallel combination of resistances in circuit theory. Since $Q(t)$ is decreasing in t, (23) gives

$$P_{\text{DA}|\gamma_{1,3},\gamma_{1,2},\gamma_{2,3}} \geq Q\left(\sqrt{(1 - \rho)\left[\gamma_{1,3} + \gamma_{\min}\right]}\right) \qquad (25)$$

Finally, averaging (25) over the exponential density functions for $\gamma_{i,j}$, we obtain a lower bound on the average error performance of diversity transmission with an amplifying relay. Using the large SNR approximations from [2], we obtain

$$P_{\text{DA}} \geq \frac{3}{K^2\,\overline{\gamma}_{1,3}\,\overline{\gamma}_{\min}}, \qquad \overline{\gamma}_{1,3}, \overline{\gamma}_{\min} \gg 1. \qquad (26)$$

In addition to the lower bound provided by (26), we can estimate the average error performance P_{DA} by computing sample averages of independent realizations of (22), or by Monte Carlo simulation of the system.

IV. PERFORMANCE SIMULATIONS

To compare performance of the transmission protocols, we examine a network with coordinates normalized by the distance $d_{1,3}$ between the source and destination radios. In these coordinates, the source can be located at $(0,0)$, and the destination can be located at $(1,0)$, without loss of generality. Due to space considerations, we limit our scope to scenarios with the relay located at $(l,0)$ for $l \approx 0$, i.e., the relay is very close to the source; $l = 1/2$, i.e., the relay is halfway between the source and destination; and $l \approx 1$, i.e., the relay is very close to the destination.

The fading variances $\sigma_{a_{i,j}}^2$ can be assigned using wireless path-loss models based on the network geometry [6]; here, we

11

utilize models of the form $\sigma_{s_{i,j}}^2 \propto d_{i,j}^{-\nu}$, where $d_{i,j}$ is the distance from mobile i to mobile j, and ν is a constant whose value, as estimated from field experiments, lies in the range $3 \leq \nu \leq 5$. Due to space considerations, we report results for $\nu = 4$, a value typical of urban environments.

To normalize for the total network energy $\mathcal{E}$ per transmitted bit, we set $\mathcal{E}_1 = \mathcal{E}$ for singlehop transmission, and $\mathcal{E}_1 = \mathcal{E}_2 = \mathcal{E}/2$ for all other transmission protocols. We plot the simulated average error performance against the singlehop average SNR. More generally, we can consider power allocations of the form $\mathcal{E}_1 = \alpha\mathcal{E}$ and $\mathcal{E}_2 = (1 - \alpha)\mathcal{E}$, and select the parameter α to minimize a variety of network performance criteria. Appropriate rate or bandwidth normalization of the results is beyond the scope of this paper.

Figs. 4–6 show simulated performance results of the various transmission protocols for uncoded BPSK transmissions, i.e., $x_0 = -1$ and $x_1 = +1$, for relay locations $(0.1, 0)$, $(0.5, 0)$, and $(0.9, 0)$, respectively. The bounds in (9) and (26) are also shown, as dashed and dashed-dotted lines, respectively, to demonstrate how well they can approximate system performance. Aside from the apparent diversity gains (decrease in slope on a log scale) for the antenna sharing protocols, multihop and antenna sharing protocols exhibit power gain (shift the curve to the left) on the order of $3(\nu - 2)$ dB for the relay located halfway between the source and destination. Note that this power gain is specific to our path-loss models.

Somewhat surprisingly, diversity transmission with an amplifying relay appears to perform comparably, if not better, than the diversity transmission schemes with a decoding relay. Characterizing this relationship more completely in various regimes will be addressed in future work.

We note that our results can, in principle, be extended naturally to multiple relays, whether employed serially or in parallel. While our analysis has been carried out strictly at the physical layer of the network in Fig. 1, obtaining the gains demonstrated in this paper requires a re-examination of the network protocol stack, at least through the traditional physical and medium-access control (MAC) layers, to provide the coordination functions required by our antenna sharing transmission protocols.

REFERENCES

[1] Thomas M. Cover and Joy A. Thomas, *Elements of Information Theory*, John Wiley & Sons, Inc., New York, 1991.

[2] John G. Proakis, *Digital Communications*, McGraw-Hill, Inc., New York, Third edition, 1995.

[3] Aradhana Narula, Mitchell D. Trott, and Gregory W. Wornell, "Performance limits of coded diversity methods for transmitter antenna arrays," *IEEE Trans. Inform. Theory*, vol. 45, no. 7, pp. 2418–2433, Nov. 1999.

[4] Fouad A. Tobagi, "Modeling and performance analysis of multihop packet radio networks," *Proc. IEEE*, vol. 75, no. 1, pp. 135–155, Jan. 1987.

[5] Andrew Sendonaris, Elza Erkip, and Behnaam Aazhang, "A novel diversity scheme for increasing the capacity of cellular systems," Submitted to tcomm, 1999.

[6] Theodore S. Rappaport, *Wireless Communications: Principles and Practice*, Prentice-Hall, Inc., Upper Saddle River, New Jersey, 1996.
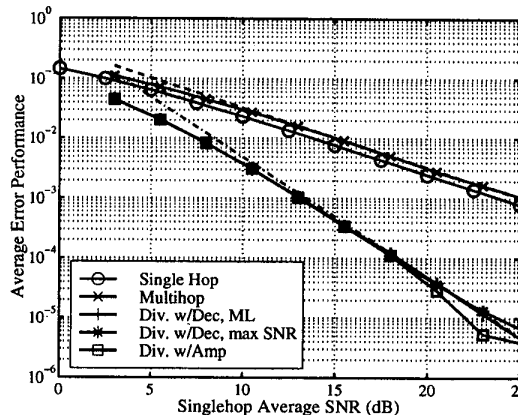
Fig. 4. Simulated performance of the transmission protocols for $\nu = 4$ and normalized geometries with the relay located at $(0.1, 0)$, i.e., close to the source.
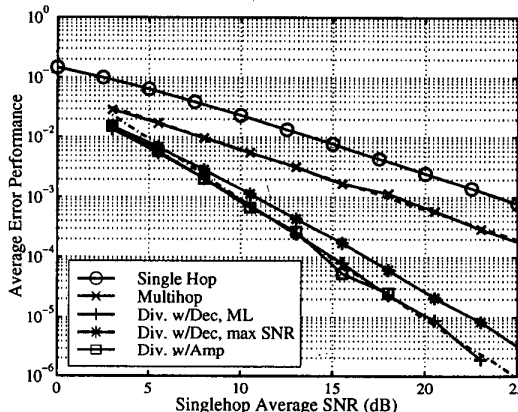

Fig. 5. Simulated performance of the transmission protocols for $\nu = 4$ and normalized geometries with the relay located at $(0.5, 0)$, i.e., halfway between the source and destination.

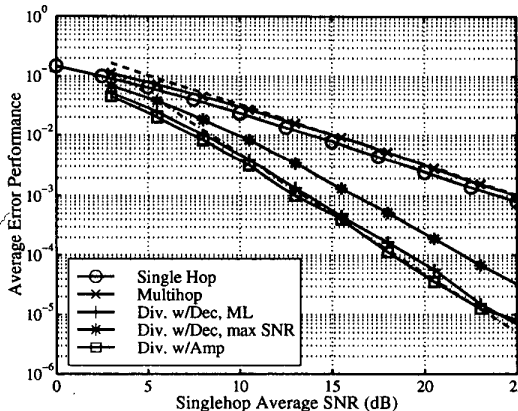Fig. 6. Simulated performance of the transmission protocols for $\nu = 4$ and normalized geometries with the relay located at $(0.9, 0)$, i.e., close to the destination.